IOP Conf. Series: Materials Science and Engineering **724** (2020) 012037 doi:10.1088/1757-899X/724/1/012037

# Erosion modelling: a systematic review of available models and equations

**A M Lospa[1,2], R G Ripeanu[1] and A Dinita[1]**

[1]Mechanical Engineering Department, Petroleum and Gas University of Ploiesti, Romania
[2]E-mail: adrian.lospa@gmail.com

**Abstract.** Across the years there was an increased attention drawn by erosion modelling, both as a general approach and also towards pipeline applications (with a concentration on pipe bends). Several authors have studied the phenomena and tried to explain the mechanisms and factors affecting the emergence and magnitude of erosion. Most of the proposed models and equations were developed for ductile materials, with a smaller part looking also at brittle materials. There are several differences observed, starting with the proposed wear mechanism and continuing with the parameters used in the equations as significant factors (for the erodent particles, target material and working conditions). The most important models and equations are analysed and presented in this article and a systematic visual representation is used to ease and simplify the understanding of the erosion modelling evolution across the years (erosion modelling in general conditions, empirical erosion modelling in pipes and bends, CFD erosion modelling in pipes and bends).

**Key words:** erosion, wear, pipe bend, erodent, pipeline

## 1. Introduction

Erosion is defined as the loss of material or loss of material integrity due to solid particle impact on the material surface [1]. Material degradation cannot be avoided, however by a proper dimensioning, material selection, use of inhibitors, by using other measures intended to reduce the erosion mechanisms or by utilizing erosion allowances, the associated effects can be minimized. Some of these measures however come with a high cost. Erosive wear can be estimated based on the speed and impact angle of the solid particles, with notable differences between ductile and brittle materials.

Salama and Venkatesh [2, 3] studied the erosion phenomena and the associated erosion mechanisms together with the parameters that are influencing the erosion rate, stating that the material erosion damage occurs as a result of the following mechanisms [2, 3]:

- Fatigue – because of cavitation (bubbles of vapours or dissolved gas collapse) or particle impingement (liquid droplet and solid particle impingement);
- Abrasive wear – as a result of repeated impingement of solid particles on ductile materials;
- Erosion – corrosion – as a result of the material protective layer deterioration by fatigue or erosive wear.

One of the most impressive studies on erosion models from 1960 to 1992 was documented by Meng and Ludema [4]. The authors checked over 5000 articles and categorized the existent equations:

- Empirical equations – developed by experimentation with varying testing conditions. This type of equations has limited validity, being more accurate than theoretical models in the testing conditions intervals. The models describe wearing under fixed sliding conditions without a proper control of testing temperature, material roughness etc.;

- Contact-mechanics-based equations – by assuming relationships between the working conditions. Many of the models are based on the assumption that one of the conventional material property (hardness, Young modulus etc.) has a big importance in the wear process;
- Equations based on material failure mechanisms.

The analysis was continued by Parsi et al. [5], taking into account also newer models (1960 – 2014). From the total of models and equations, only a part has been presented based on [4, 5]:

- Author's maturity – measured by the length of time the author has published papers and research on erosion and by how many times it was cited by other authors;
- Equation logical consistency – a reasonable and detailed explanation for the derivation of the wear equations from the initial assumptions to the final expressions;
- Historical significance and continuations of the proposed model.

In this article, the authors want to review the available erosion models that were proposed along the years, to understand the conditions in which the models were obtained, the parameters that were used as predictors in the equations and the applicability.

## 2. General equations and models developed for erosion phenomena analysis

Model 1 - Finnie [6] studied erosion by solid particles in case of ductile materials, for low impingement angles ($\alpha < 45°$). There is a power law between the volume of removed material and the solid particle velocity, with an exponent of 2. He proposed equations (2) and (3) to determine the erosion produced by a single erodent particle, for different impingement angles.

$$\varepsilon_{VP} = \frac{MV_p^2}{P} f(\alpha) \quad (1) \qquad \varepsilon_{VP} = \frac{mV^2}{P\Psi\kappa}\left(\sin(2\alpha) - \frac{6}{\kappa}\sin^2\alpha\right), \ \tan\alpha \le \frac{k}{6} \quad (2) \qquad \varepsilon_{VP} = \frac{mV^2}{P\Psi\kappa}\frac{\kappa\cos^2\alpha}{6}, \ \tan\alpha \ge \frac{k}{6} \quad (3)$$

Model 2 - Bitter [7] studied erosion in fluid-bed systems, assuming two wear mechanisms, deformation because of repeated solid particle collision and cutting of the free-moving particles:

$$\varepsilon_{VT} = \varepsilon_{VP} + \varepsilon_{VC} \quad (4) \qquad \varepsilon_{VC1} = \frac{2MV_p\left(V_p\sin\alpha - K\right)^2}{\left(V_p\sin\alpha\right)^{\frac{1}{2}}}\left(V_p\cos\alpha - \frac{C\left(V_p\sin\alpha - K\right)^2}{\left(V_p\sin\alpha\right)^{\frac{1}{2}}}\chi\right), \ \alpha \le \alpha_{p0} \quad (6)$$

$$\varepsilon_{VP} = \frac{1}{2}\frac{M\left(V_p\sin\alpha - K\right)^2}{\delta} \quad (5) \qquad \varepsilon_{VC2} = \frac{\frac{1}{2}M\left(V_p^2\cos^2\alpha - K_1\left(V_p\sin\alpha - K\right)^{3/2}\right)}{\chi}, \ \alpha \ge \alpha_{p0} \quad (7)$$

Model 3 - Sheldon and Finnie [8] studied the erosive cutting of a brittle material by the normal impact of a stream of solid particles (angular silicon carbide particles and spherical steel shot):

$$\varepsilon_{VP} = K_4 r^a V_p^b, \ a = \frac{3n}{n-2}, \ b = \frac{2.4n}{n-2} \quad (8) \qquad \varepsilon_{VC} = K_5 r^{a'} V_p^b, \ a' = \frac{3.6n}{n-2}, \ b = \frac{2.4n}{n-2} \quad (9) \qquad K_5 = \frac{K_4}{r^{0.6n/(n-2)}} \quad (11)$$

$$K_4 = C_2\pi\left(\frac{K_3}{K_2}\right)^{2n/(n-2)}\left(\frac{5\pi}{3}\right)^{1.2n/(n-2)}\left(\frac{\rho_p}{\gamma^2}\right)^{1.2n/(n-2)} \quad (10) \qquad K_3 = \frac{1-2\upsilon}{4\pi} \quad (12) \qquad K_2 = \sigma_b V_b^{1/n}\left(\frac{n-1}{4\pi\left(n+1\right)K_1}\right)^{1/n} \quad (13)$$

Model 4 - Neilson and Gilchrist [9] determined the erosive action of a particle laden gas stream on specimen materials with different physical properties, assuming that the normal component of the solid particle kinetic energy is causing deformation wear, with the parallel component causing cutting wear:

$$\varepsilon_V = \frac{1}{2}\frac{M\left(V_p^2\cos^2\alpha - V_r^2\right)}{\chi} + \frac{1}{2}\frac{M\left(V_p\sin\alpha - K\right)^2}{\delta}, \ \alpha < \alpha_{p0} \quad (14) \qquad \varepsilon_V = \frac{1}{2}\frac{MV_p^2\cos^2\alpha}{\chi} + \frac{1}{2}\frac{M\left(V_p\sin\alpha - K\right)^2}{\delta}, \ \alpha > \alpha_{p0} \quad (15)$$

Model 5 - Goodwin, Sage and Tilly [10] have studied the influence of solid particle velocity, erodent type and particle fragmenting on the erosion of ductile materials. For sand particles, the most important factors are the particle size and quartz concentration. For industrial erodent particles, the most important characteristics are particle hardness and particle sharpness.

$$\varepsilon_m = K_1 V^a \quad (16) \qquad a = 2 \text{ for } 25\mu\text{m and } a = 2.3 \text{ for } 125\mu\text{m}$$

Model 6 - Head and Harr [11] developed statistical models for erosion on ductile and brittle target materials. The main factor is represented by the energy transmitted from the erodent particles to the target material. Erosion develops only when a threshold value of the transmitted energy is reached.

$$\varepsilon_{V(DW)} = 0.000233 - 0.000160R - 0.000238\ln\left(\frac{H_p}{E_{re}}\right) - 0.000210\ln\left(\frac{H_t}{E_{re}}\right) + 0.001577\left(\frac{V^2}{E_{re}}\right) + 0.00829\sin\alpha + 0.000034\left[\ln\left(\frac{H_p}{E_{re}}\right)\right]^2 - 0.000967\left(\frac{V^2}{E_{re}}\right)^2 R \quad (17)$$

$$+ 0.000119R\ln\left(\frac{H_t}{E_{re}}\right) - 0.001380\ln\left(\frac{H_t}{E_{re}}\right)\cos\alpha + 0.0001456\left[\ln\left(\frac{H_p}{E_{re}}\right)\right]^2\cos\alpha$$

$$\varepsilon_{V(BW)} = 0.005345 + 0.000006\frac{V^2}{E_{re}} + 0.003507R + 0.009335\sin\alpha - 0.000630\ln\left(\frac{H_p}{E_{re}}\right) - 0.004706\cos\alpha - 0.003114\sin^2\alpha - 0.010888\sin\alpha \quad (18)$$

$$- 0.003810R\cos\alpha + 0.000495\ln\left(\frac{H_t}{E_{re}}\right)\cos\alpha$$

$$\varepsilon_{V(BS)} = \frac{V^{3.06}\alpha^{2.69}H_p^{2.08}E_{re}^{0.03}}{H_t^{2.08}} \quad (19)$$

$$\varepsilon_{V(DS)} = \frac{V^{4.34}\alpha^{0.46}H_p^{0.10}E_{re}^{0.21}}{R^{2.48}H_t^{2.48}} \quad (20)$$

Model 7 – Sheldon [12] studied solid particle erosion for ductile and brittle materials and acknowledged the erosion dependence on particle diameter and velocity and target material properties.

$$W = K_1 r^a V^b \quad (21) \qquad K_1 = \frac{E^{0.8(n+1)/(n-2)}}{\sigma_0^{2n/(n-2)}} m^{1.2(n-0.67/(n-2)} \quad (22) \qquad a = \frac{3(n-0.67)}{n-2} \quad (23) \qquad b = 2.4\frac{n-0.67}{n-2} \quad (24)$$

Model 8 – Finnie [13] has resolved the motion equation for an erodent particle and proposed the following expression to determine the erosion rate:

$$\varepsilon_V = \frac{cMV_p^2}{4P\left(1+\frac{m_p r^2}{I}\right)}\left[\cos^2(\alpha) - \left(\frac{\dot{x}_t'}{V_p}\right)^2\right] \quad (25) \qquad \dot{x}_t' = V_p\cos\alpha - \frac{2V_p}{P}\sin\alpha \quad (26)$$

Model 9 – Sheldon and Kanhere [14] investigated the effect of a high dimension erodent particle on aluminium surfaces by material displacement followed by material breakage due to existing efforts.

$$\varepsilon_{VP} = \frac{d_p^3 V_p^3 \rho_p^{3/2}}{H_V^{3/2}} \quad (27)$$

Model 10 – Tilly [15] continued the research on ductile materials and acknowledged the existence of two stages: indentation and/or breakage of material because of solid particle repeated impact on the surface and the material wear because of particle fragments generated in the first stage.

$$\varepsilon_V = \hat{\varepsilon}_1\left(\frac{V_p}{V_{ref}}\right)^2\left[1-\left(\frac{d_0}{d_p}\right)^{3/2}\frac{V_0}{V_p}\right]^2 + \hat{\varepsilon}_2\left(\frac{V_p}{V_{ref}}\right)^2 F_{d,v} \quad (28) \qquad \hat{\varepsilon}_2 = \varepsilon_V - \hat{\varepsilon}_1 \quad (29) \qquad F_{d,v} = \frac{W_0 - W}{W_0} \quad (30)$$

Model 11 – Head, Lineback and Manning [16] derived the previous proposed model to take into account also higher speeds of the solid particles (3000 m/s).

$$\varepsilon_{V(DMW)}(\alpha) = \left|\frac{\varepsilon_{V(DW)}(\alpha_0) - \varepsilon_{V(DW)}(\alpha)}{F}\right| \quad (31)$$

Model 12 - Grant and Tabakoff [17] determined the erosion behaviour for Aluminium 2024.

$$\varepsilon_V = K_1\left\{1+C\left[K_2\sin\left(\frac{90}{\alpha_0}\alpha\right)\right]\right\}^2 V_p^2\cos^2\alpha\left(1-R_T^2\right)+K_3\left(V_p\sin\alpha\right)^4 \quad (32)$$

$$\begin{matrix} C=1,\ \alpha\le 3\alpha_0 \\ C=0,\ \alpha>3\alpha_0 \end{matrix} \quad (33)$$

Model 13 - Williams and Lau [18] studied the erosion mechanism for epoxy graphite composites.

$$\varepsilon_V = K_1 d^a\left[V_p\sin\left(\alpha+K_2\right)\right]^b \quad (34)$$

Model 14 - Jennings, Head and Manning [19] established that the erosion mechanism develops because of superficial melting of the ductile target material at the solid particle impact.

$$\varepsilon_V = \frac{K_T^{5/2}}{R}\frac{G^{1/3}}{\rho_t^{1/3}kT_m\Delta H_m} \quad (35)$$

Model 15 - Hutchings, Winter and Field [20] experimentally determined the erosion produced by spherical metallic particles at the oblique impact on mild steels, crater dimensions depending on the particle impingement angle and speed.

$$\varepsilon_m = 5.82\times10^{-10}V_p^{2.9} \quad (36)$$

Model 16 – Finnie [21] proposed two methods by which the cutting mechanism is finalized: when the particle tip cannot advance, the speed horizontal component becoming zero and when the particle tip leaves the material surface, while the particle still moves on horizontal trajectory.

$$\varepsilon_V = \frac{cMV_p^2}{4P\left(1+\frac{m_p r^2}{I}\right)}\cos^2\left(\alpha\right);\ \dot{x}_t' = 0,\ \alpha\ge\tan^{-1}\frac{p}{2} \quad (37)$$

$$\varepsilon_V = \frac{cMV_p^2}{4P\left(1+\frac{m_p r^2}{I}\right)}\left[\sin 2\alpha - 2\frac{\sin^2\alpha}{p}\right];\ y_t = 0,\ \alpha\le\tan^{-1}\frac{p}{2} \quad (38)$$

Model 17 – Evans, Gulden and Rosenblatt [22] studied the wear phenomena for brittle materials based on an elastic-plastic response, the radial cracks formation determining the affected area increase and the lateral cracks formation determining the material penetration.

$$\varepsilon_{VP} \propto \frac{V_p^{19/6} r^{11/3}\rho_p^{1/4}}{K_c^{4/3}H_t^{1/4}} \quad (39)$$

Model 18 – Evans [23] proposed a new equation for brittle materials.

$$\varepsilon_{VP} \propto \frac{\left(\rho_p\rho_t\mu_p\mu_t\right)^{2/3}}{\left[\left(\rho_p\mu_p\right)^{1/2}+\left(\rho_t\mu_t\right)^{1/2}\right]^{8/3}}\rho_p^{19/12} r^{11/3}V_p^{19/6}K_c^{-4/3}H_t^{-1/4} \quad (40)$$

Model 19 - Ruff and Wiederhorn [24] proposed an equation to determine erosion for brittle materials.

$$\varepsilon_{VP} \propto \frac{\left(\rho_p\rho_t\mu_p\mu_t\right)^{2/3}}{\left[\left(\rho_p\mu_p\right)^{1/2}+\left(\rho_t\mu_t\right)^{1/2}\right]^{8/3}}\rho_p^{11/19} r^{11/3}V_p^{22/9}K_c^{-4/3}H_t^{1/9} \quad (41)$$

Model 20 - Tabakoff, Kotwal and Hamed [25] developed a semi-empirical model to determine the erosion rate for various impingement angles and speed of ash particles.

$$\varepsilon_m = K_1 f\left(\alpha\right)V_p^2\left(\cos^2\alpha\right)\left(1-e_t^2\right)+f\left(V_p,n\right) \quad (42)$$

$$e_t = 1-0.0016V_p\sin\alpha \quad (43)$$

$$f\left(\alpha\right) = \left\{1+K_4\left[K_2\sin\left(\frac{\pi}{2}\frac{\alpha}{\alpha_m}\right)\right]\right\}^2 \quad (44)$$

$$f\left(V_p,n\right) = K_3\left(V_p\sin\alpha\right)^4 \quad (45)$$

$$\begin{matrix} K_4=1,\ \alpha\le 3\alpha_m \\ K_4=0,\ \alpha>3\alpha_m \end{matrix} \quad (46)$$

Model 21 - Routbort, Scattergood and Turner [26] determined the erosion for siliconized silicon carbide SiSiC at the impact with $Al_2O_3$ particles, with dimensions of 23 - 270 μm, speeds of 54 – 151 m/s and impingement angles of 10 - 90°.

$$\varepsilon_m = r^{0.7-0.95}V_p^{2.0-2.5} \quad (47)$$

Model 22 - Routbort, Scattergood and Kay [27] continued the research and determined the erosion for siliconized silicon carbide SiSiC at the impact with sharp $Al_2O_3$ particles, with dimensions of 23 - 270 μm, speeds of 32 – 134 m/s and impingement angles of 22 - 90°.

$$\varepsilon_m = \left(V_p \sin\alpha - V_0\right)^n \left(d - d_0\right)^m \tag{48}$$

Model 23 – Hutchings [28] performed a theoretical analysis for the erosion of aluminium alloys at the normal impact of spherical steel shots.

$$\varepsilon_m = 0.033 \frac{\alpha \rho_t P^{1/2} V_p^3}{\Omega_c^2 H_t^{3/2}} \tag{49}$$

Model 24 - Sundarajan and Shewmon [29] proposed an erosion model based on a localization concept (the lip formation is the result of localization of deformation in the near-surface regions of the target and is removed either by inertial-stress-induced tensile fracture or by separation across shear bands).

$$\varepsilon_m = \frac{0.085 V_p^{2.5} \rho_p^{1/4} \rho_t^{1-b} \alpha \left(z+1\right)^{5a} \left[1 - \left(z+1\right)/\left(z+2\right)\right] F\left(z\right)}{6.06^b \left(1 - CT_c\right)^{1.5} \left[n_c C_p T_m^{0.75} \left(1 - 436/T_m\right)^{0.75}\right]^b \left(K_1 H_t\right)^{1.25-b}} \tag{50}$$

$$a = \frac{0.25 n_c^{1-a_1 S} \left(z+1\right)^S \left(K_1 H_t\right)^{a_1 S}}{\left[6.06 \rho_t C_p T_m^{0.75} \left(1 - 436/T_m\right)^{0.75}\right]^{a_1 S}} \tag{51}$$

$$b = \left(1 + 5a\right) a_1 \tag{52}$$

Model 25 – Beckmann and Gotzmann [30] tested the hypothesis by which the volume of removed material in case of abrasive wear is proportional with the shear stress generated in the affected region.

$$\varepsilon_m = \left[\tau_0 + \left(\frac{\varphi}{2}\right)^{1/2} H\right] \varphi^{5/2} \cos^2\alpha \sin^{1/2}\alpha + \left(\tau_0 + \left(\frac{2\varphi}{1-\varphi}\right)^{1/2} H\right) \varphi^2 \sin^2\alpha \tag{53}$$

$$\varphi = V \left(\frac{2\rho}{3H}\right)^{1/2} \tag{54}$$

Model 26 - Wiederhorn and Hockey [31] determined the erosion for brittle materials.

$$\varepsilon_m \propto V_p^{2.8} r^{3.9} \rho_p^{1/4} K_c^{-1.9} H_t^{0.48} \tag{55}$$

Model 27 – Ritter [32] studied the ceramic materials erosion response at the impact with $Al_2O_3$, SiC, $Si_3N_4$ and MgO particles, stating that material wear is dependent upon the solid particle kinetic energy.

$$\varepsilon_m \propto \frac{d_\gamma E U_k}{K_c^2} \tag{56}$$

Model 28 – Reddy and Sundarajan [33] determined experimentally that the main erosion mechanism consists of a lip formation at the solid particle impact on the target material followed by tearing and this generating material removal.

$$\varepsilon_{VP} \propto \frac{L^3 \Delta\Omega_m}{\Omega_c} \tag{57}$$

Model 29 – Johansson, Ericson and Schweitz [34] developed a statistical model to determine the erosion rate for single-crystal semiconductors.

$$\varepsilon_m = \left(1 - f\right) K_1 \frac{\rho_t \rho_p^{2.9} E_t^{2/3} V_p^{22/9} d_p^{2/3}}{H_t^{5/9} K_c^{4/3}} + f K_2 \frac{\rho_t \rho_p^{1/3} E_t V_p^{8/3} d_p}{H_t^{1/3} K_c^2} \tag{58}$$

Model 30 – Lhym and Wapner [35] studied erosive wear on PPS composite materials.

$$\varepsilon_m = K_1 K_c^{a-2} V_p^{5-2b} d_p^{6K_2} \rho_t^2 \rho_p \tag{59}$$

Model 31 – Sundarajan [36] proposed a new model for ductile material erosion that takes into account the whole range of impingement angles and various dimensions of the erodent particles.

$$\varepsilon_m = \left(2^{n_h} C V_p^2 \sin^2\alpha F\left(t\right) / \left(n_h C_p\right)\right) \left\{1 + \left[\left(n_h + 1\right)\left(\frac{\mu}{\mu_c}\right)\left(2 - \left(\frac{\mu}{\mu_c}\right)\right) \Big/ 4\left(1+\lambda\right)\tan^2\alpha F\left(t\right)\right] - e^2\right\} \tag{60}$$

$$e = \frac{1.9H_p^{5/8}}{E_e^{1/2}\rho_p^{1/8}V_p^{1/4}} \quad (61) \qquad F(t) \approx 0.02 - 0.05 \quad (62)$$

Model 32 – Ahlert [37] proposed an empirical correlation to determine the erosion rate for carbon steels with wet or dry surfaces.

$$\varepsilon_m = 2.17\times10^{-7}\times(BH)^{-0.59}F_sV_p^{2.41}F(\alpha) \quad (63) \qquad F(\alpha) = \sum_{i=1}^{5} A_i\alpha^i \quad (64)$$

Model 33 – Haugen et al. [38] studied the erosion from choke valves used in the oil and gas industry.

$$\varepsilon_m = MK_pF(\alpha)V_p^{np} \quad (65)$$

Model 34 – Chen et al. [39] proposed an erosion model for the normal impact of solid particles based on a residual tensile stress mechanism.

$$\varepsilon_m = 0.064\frac{\rho_t\rho_pV_p^3}{\bar{p}^{3/2}\left[D_1 + D_2\exp\left(D_3\sigma^*\right)\right]^2\left[1 + D_4\ln\dot{\varepsilon}^*\right]^2\left(1 + D_5T^*\right)^2} \quad (66)$$

Model 35 – Chen et al. [40] continued the research and proposed a new general model based on the friction generated at particle impact.

$$\varepsilon_D = \frac{T_y}{m_p\delta} = \frac{\sum m_pV_{pn}\Delta V_{pn}}{m_p\delta} \quad (67) \qquad \varepsilon_C = \frac{T_\chi}{m_p\chi} = \frac{\sum m_pV_{pt}\Delta V_{pt}}{m_p\delta\chi} \quad (68) \qquad T_t = T_y + T_\chi \quad (61) \qquad \varepsilon_V = \varepsilon_C + \varepsilon_D \quad (69)$$

Model 36 – Levin et al. [41] developed an erosion model that takes into account the mechanical properties of the target material and the hardening effect at the particle impact.

$$\varepsilon_m \propto \frac{m_pV_p^2}{2}\left\{\frac{\left[1 - \left(\frac{3.06H_t^{5/4}}{\rho_pV_p^{1/2}}\right)\left(\frac{1-\mu_t^2}{E_t} + \frac{1-\mu_p^2}{E_p}\right)\right]}{T\cdot L_V}\right\} \quad (70)$$

Model 37 – Oka et al. [42] proposed an erosion model that considers the mechanical properties of the target material and the impact parameters. The model includes the repeated plastic deformation of the target material because of normal particle impact and the cutting process generated at low impingement angles.

$$\varepsilon(\alpha) = f(\alpha)\varepsilon_{90} \quad (71) \qquad f(\alpha) = (\sin\alpha)^{n_1}(1 + H_V(1-\sin\alpha))^{n_2} \quad (72) \qquad \varepsilon_{90} = K_p(H_V)^{k_1}(V_p)^{k_2}(d_p\times10^{-6})^{k_3} \quad (73)$$

Model 38 – Oka et al. [43] modified the previous proposed model for a better correlation.

$$\varepsilon(\alpha) = f(\alpha)\varepsilon_{90} \quad (74) \qquad f(\alpha) = (\sin\alpha)^{n_1}(1 + H_V(1-\sin\alpha))^{n_2} \quad (75) \qquad \varepsilon_{90} = K_p(k_4H_V)^{k_1b}\left(\frac{V_p}{v}\right)^{k_2}\left(\frac{d}{r}\right)^{k_3} \quad (76)$$

Model 39 – Huang et al. [44] developed a phenomenological model to determine the erosion, assuming that particle impact generating normal and tangential forces determines material deformation.

$$\varepsilon_{VT} = \varepsilon_{VC} + \varepsilon_{VD} \quad (77) \qquad \varepsilon_{VD} = C_1\frac{m_p\rho_p^{1/4b'}\left(V_p\sin\alpha\right)^{2+(1/2b')}}{\varepsilon_c^{1/b'}p_n^{1+(1/4b')}} \quad (78)$$

$$\varepsilon_{VC} = \frac{C_2m_p^{1+[3(1-n_s)/4)]}V_p^{2+[3(1-n_s)/2)]}\left(\cos\alpha\right)^2\left(\sin\alpha\right)^{[3(1-n_s)/2)]}}{d_p^{(1-n_s)/4)}\varepsilon_0^{i}p_t^{3(1-n_s)/4)}p_n^{3(1-n_s)/4)}} \quad (79)$$

Model 40 – Nsoesie et al. [45] studied the erosion mechanism for five Stellite alloys.

$$\varepsilon_V = \frac{C_1d_p^3\left(V_p\left(A\left(\sin\left(\alpha/2\right)^{1/3}\right)\right)^B\right)^3\rho_p^{3/2}}{H_V^{3/2}} \quad (80)$$

## 3. Empirical equations and models developed for erosion phenomena analysis in pipe bends

Model 41 – API RP 14E [46] – as per the standard, to prevent the apparition of erosion phenomena, it is recommended to have a threshold for the flow velocity when designing the piping or pipeline system.

$$V_e = \frac{C}{\sqrt{\rho_m}} \tag{81}$$

Model 42 – Salama and Venkatesh [47] studied the limitation of the API RP 14E model, considering that the approach is conservative based on experimental testing and proposed the following equation:

$$V_e = \frac{300}{\sqrt{\rho_m}} \tag{82}$$

Model 43 – Salama and Venkatesh [48] continued the experimental testing and based on the results of Rabinowicz [49] proposed the following model for pipe bends. The model is conservative and overestimates the experimental results with a factor of 1.44.

$$ER = 1.86 \cdot 10^5 \frac{W_p V_f^2}{PD^2} \tag{83}$$

Model 44 – Bourgoyne [50] suggested two equations to determine the erosion rate, one for gas conveying systems (74), and the other for liquid flows (75).

$$ER = F_e \frac{\rho_p}{\rho_t} \frac{W_p}{A} \left( \frac{V_{SG}}{100\alpha_g} \right)^2 \tag{84}$$

$$ER = F_e \frac{\rho_p}{\rho_t} \frac{W_p}{A} \left( \frac{V_{SL}}{100H_L} \right)^2 \tag{85}$$

Model 45 – Svedman et al. [51] studied the applicability of Bourgoyne's model for low speed flows and suggested an equation to limit the flow speed in order to limit the tolerable erosion rate at 5 MPY.

$$V_e = K_S \frac{D}{\sqrt{W_p}} \tag{86}$$

$$K_S = 1.34 \text{ for long radius elbows} \qquad K_S = 7.04 \text{ for tees} \tag{87}$$

Model 46 – Jordan [52] also proposed a model for erosion rate calculation.

$$ER = 10^{C_1} V_{SG}^{2.349} W_p^{0.9535} \left( 1 - \left( 1 + \frac{1}{2r_c} \right)^{-2} \right)^{1.885/2} \tag{88}$$

Model 47 – McLaury and Shirazi [53] from Tulsa University E/CRC – Erosion/Corossion Research Centre proposed a semi-empirical model to calculate erosion in pipe bends and tees.

$$ER = F_M F_S F_P F_{r/D} \frac{W_p V_L^n}{\left( D/D_0 \right)^2} \tag{89}$$

Model 48 – DNVGL-RP-O501 [54] - as per the standard, the following relations can be used for erosion rate calculation in straight pipes (90) and in pipe bends (91).

$$E_{L,y} = 2.5 \cdot 10^{-5} \cdot U_p^{2.6} \cdot D^{-2} \cdot m_p \tag{90}$$

$$E = \frac{K \cdot U_p^n \cdot F(\alpha)}{\rho_t \cdot A_t} \cdot G \cdot C_1 \cdot GF \cdot M_p \cdot 10^3 \tag{91}$$

## 4. Systematic representation of available wear models and equations

The authors came up with a visual representation of all the discussed erosion models, both general and empirical for pipe bends. Taking some ideas from the periodic table of elements, the models are represented based on number, author name, year, plus details related to the parameters used in the equations. There are three criteria used for parameter categorization, solid particle material properties, target material properties and experimental working conditions. For the cases where the authors

contributed with more than one model, the same colour is used. The "Periodic table of erosion models" can be amended whenever a new model arises that ensures the conditions from the first section.

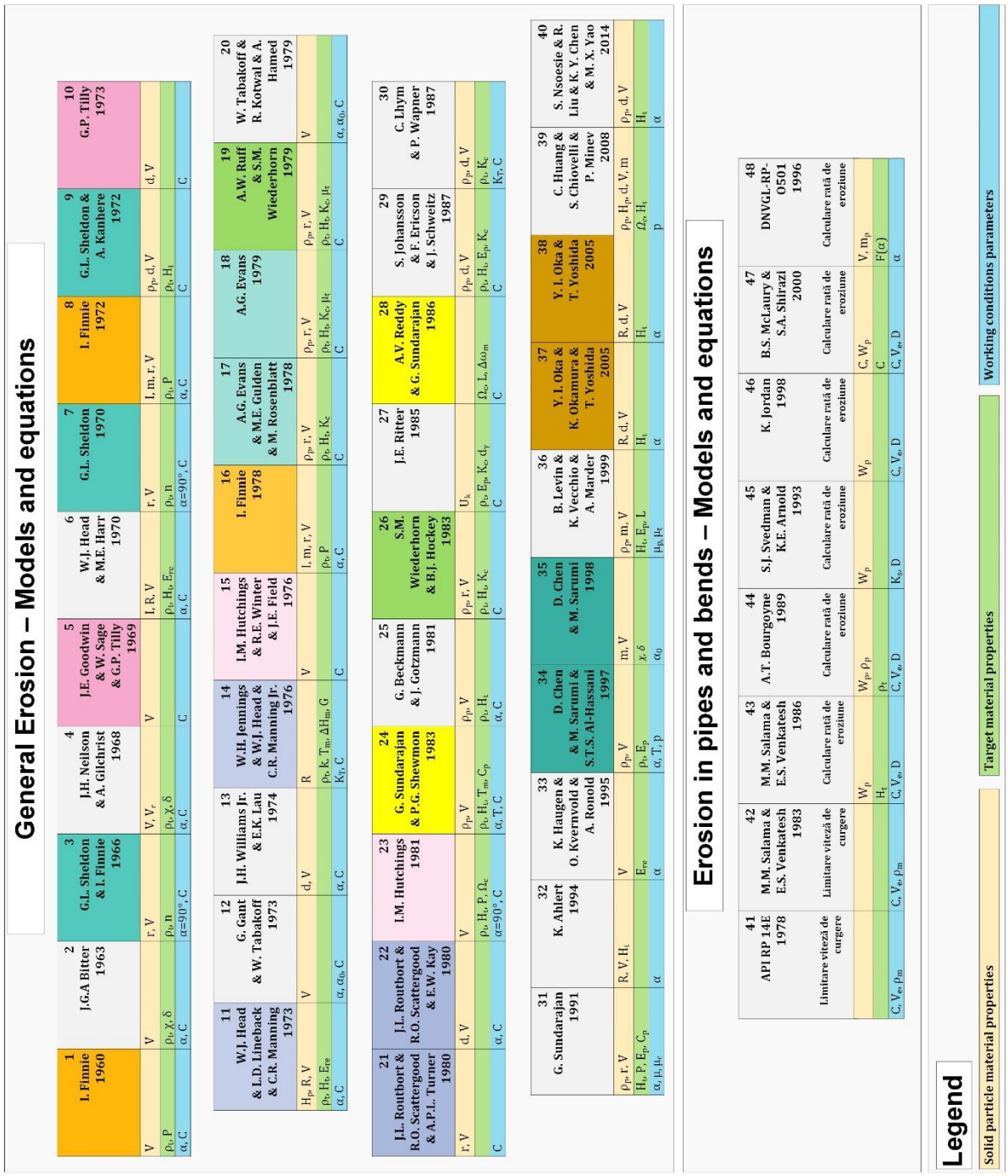


**Figure 1.** Periodic table of erosion models

The parameters from the "Periodic table of erosion models" have the following meaning: $\rho_p$ – *particle density;* $H_p$ – *particle hardness;* $I$ – *moment of inertia;* $R$ – *particle circularity;* $m$ – *particle mass;* $d$ – *particle diameter;* $r$ – *particle radius;* $V$ – *particle speed;* $V_r$ - *rebound speed;* $U_k$ - *kinetic energy;* $\rho_t$ – *material density;* $H_t$ – *material hardness;* $P$ – *flow stress;* $E_p$ - *Young's modulus;* $K_c$ – *fracture toughness;* $\Omega_c$ – *critical strain;* $L$ – *depth of deformation;* $\Delta\omega_m$ – *incremental strain per impact;* $k$ – *thermal conductivity;* $T_m$ – *melting temperature;* $\Delta H_m$ - *enthalpy of melting;* $\chi$ – *cutting energy;* $\delta$ – *deformation energy;* $E_{re}$ – *erosion resistance;* $C_p$ – *heat capacity;* $G$ - *grain molecular weight;* $n$ - *Weibull flaw*

*parameter; $\mu_t$ - Lame constant; $d_\gamma$ - grain diameter; $\mu$ - friction coefficient; $\mu_c$ - Critical friction coefficient; $\mu_p$ - Poisson coefficient; $\mu_t$ - critical Poisson coefficient; $\alpha$ - Impingement angle; $\alpha_0$ - maximum wear impingement angle; $K_T$ - Kinetic energy transfer from particle to target; T – temperature; p – pressure; C – different constants.*

## 5. Conclusions

The presented models have an average of 6 parameters as factors in the equations, the highest number of parameters being 11 and the lowest 2. 28 of the models take into account the working conditions by incorporating different constants and 23 out of them have included the impingement angle of the solid particles in the relations. 37 models are factoring the solid particle speed, 20 of them the particle dimension and 14 of them the particle density. 22 models included the target material density, 17 of them the target material hardness and 7 of them the fracture toughness. All the models provide acceptable results with specific materials and working conditions as per the experimental conditions, however they lack a general applicability.

For pipeline practical applications, in case of complex geometrical layouts or when the exact location of the erosion attack is important it is recommended to use Computational Fluid Analysis (CFD). There is no convergence between the models proposed by the above-mentioned authors, the parameters used as factors being quite different between equations. This shows a need for further research by looking at what parameters are really important in the erosion phenomena. The "Periodic table of erosion models" will be further amended in future work with the models used in various commercial CFD software.

## 6. References

[1] Det Norske Vertitas 2015 Recommended practice DNVGL-RP-O501 Managing sand production and erosion
[2] Salama M M and Venkatesh E S 1983 *15th Annual Offshore Technol. Conf. Houston Texas* pp 371 – 376
[3] Venkatesh E S 1986 *Proc. Rocky Mountain Meeting of SPE Billings MT* pp 489-497
[4] Meng H C, Ludema K C 1995 *Wear* **181–183(2)** pp 443-457
[5] Parsi M, Najmi K, Najafifard F, Hassani S, McLaury B S and Shirazi S A 2014 *J. Nat. Gas Sci. Eng.* **21** pp 850-873
[6] Finnie I 1960 *Wear* **3(2)** pp 87-103
[7] Bitter J G A 1963 *Wear* **6(1)** pp 5-21
[8] Sheldon G L and Finnie I 1966 *J. Energ. Resour. -ASME* **88(4)** pp 393-399
[9] Neilson J H and Gilchrist A 1968 *Wear* **11(2)** pp 111-122
[10] Goodwin E, Sage J and Tilly W P 1969 *Proc. Inst. Mech. Eng.* 1-196 pp 279-292
[11] Head W J, Harr M E 1970 *Wear* **15(1)** pp 1-46
[12] Sheldon G L 1970 Similarities and differences in the erosion behaviour of materials *J. Basic Eng.*
[13] Finnie I 1972 *Wear* **19(1)** pp 81-90
[14] Sheldon G L and Kanhere A 1972 *Wear* **21(1)** pp 195-209
[15] Tilly G P 1973 *Wear* **23(1)** pp 87-96
[16] Head W J, Lineback L D and Manning C R 1973 *Wear* **23(3)** pp 291-298
[17] Grant G and Tabakoff W 1973 An experimental investigation of the erosive characteristics of 2024 aluminium alloy *Dept. of Aerospace Eng. Univ. Cincinnati*
[18] Williams J H and Lau E K 1974 *Wear* **29(2)** pp 219-230
[19] Jennings W H, Head W J and Manning C R 1976 *Wear* **40(1)** pp 93-112
[20] Hutchings I M, Winter R E and Field J E 1976 *P. Roy. Soc. A-Math. Phy.* **348(1654)** pp. 379-392
[21] Finnie I, McFadden D H 1978 *Wear* **48(1)** pp 181-190
[22] Evans A G, Gulden M E and Rosenblatt M 1978 *P. Roy. Soc. A-Math. Phy.* **361(1706)** pp. 343-365
[23] Evans A G 1979 *Treatise on Mater. Sci. Technol.* **16** pp. 1-67
[24] Ruff A W and Wiederhorn S M 1979 Erosion by solid particle impact *National bureau of standards Gaithersburg md national measurement lab*
[25] Tabakoff W, Kotwal R and Hamed A 1979 *Wear* **52(1)** pp 161-173

[26] Routbort J L, Scattergood R O and Turner A P L 1980 *Wear* **59(2)** pp 363-375
[27] Routbort J L, Scattergood R O and Kay E W 1980 *J Am. Ceram. Soc.* **63** pp 635-640
[28] Hutchings I M 1981 *Wear* **70(3)** pp 269-281
[29] Sundararajan G and Shewmon P G 1983 *Wear* **84(2)** pp 237-258
[30] Beckmann G and Gotzmann J 1981 *Wear* **73(2)** pp 325-353
[31] Wiederhorn S M and Hockey B J 1983 *J. Mater. Sci.* **18(3)** pp 766-780
[32] Ritter J E 1985 *Mater. Sci. Eng.* **71** pp 195-201
[33] Reddy A V and Sundararajan G 1986 *Wear* **111(3)** pp 313-323
[34] Johansson S, Ericson F and Schweitz J 1987 *Wear* **115(1-2)** pp 107-120
[35] C. Lhymn C and Wapner P 1987 *Wear* **119(1)** pp 1-11
[36] Sundararajan G 1991 *Wear* **149(1-2)** pp 111-127
[37] Ahlert K 1994 *M. Sc. Thesis Dept. Mech. Eng. Univ. Tulsa*
[38] Haugen K, Kvernvold O, Ronold A and Sandberg R 1995 *Wear* **186–187**(1) pp 179-188
[39] Chen D, Sarumi M, Al-Hassani S T S, Gan S and Yin Z 1997 *Wear* **205(1–2)** pp 32-39
[40] Chen D, Sarumi M and Al-Hassani S T S 1998 *Wear* **214(1)** pp 64-73
[41] Levin B, Vecchio K and Marder A 1999 *Metall. Mater. Trans. A 30A* pp 1763-1774
[42] Oka Y I Okamura K and Yoshida T 2005 *Wear* **259(1–6)** pp 95-101
[43] Oka Y I and Yoshida T 2005 *Wear* **259(1–6)** pp 102-109
[44] Huang C et al. 2008 *Powder Technol.* **187(3)** pp 273-279
[45] Nsoesie S, Liu R, Chen K Y and Yao M X 2014 *Wear* **309(1–2)** pp 226-232
[46] API 14E Recommended practice for design and installation of offshore production platform piping systems 5th edition 1991 (revised 2000)
[47] Salama M M, and Venkatesh E S 1983 Evaluation of API RP 14E erosional velocity limitations for offshore gas wells *Offshore Technol. Conf*
[48] Venkatesh E S 1986 Erosion damage in oil and gas wells *Proc. Rocky Mountain Meeting of SPE Billings MT*
[49] Rabinowicz E 1979 *Intl. Conf. on Erosion by Liquid and Solid Impact 5th Cambridge England* pp. 38-1
[50] Bourgoyne A T 1989 Experimental study of erosion in diverter systems due to sand production *SPE*
[51] Svedeman S J and Arnold K E 1993 Criteria for sizing multiphase flow lines for erosive-corrosive service *Proc. of 68th SPE Annual Fall Technical Conf. Houston*
[52] Jordan K 1998 Erosion in multiphase production of oil & gas corrosion *NACE Intl. Annual Conf. San Antonio*
[53] Shirazi S A, Shadley J R, McLaury B S and Rybicki E F 1995 *J. Press. Vess. - T. ASME* **117 (1995)** pp 45-52
[54] McLaury B S and Shirazi S A 2000 *J. Energ. Resour. - ASME* **122** pp 115-122